nature communications

Article

https://doi.org/10.1038/s41467-025-59583-8

High-efficiency and long-lifetime deep-blue phosphorescent OLEDs using deuterated exciplex-forming host

Received: 15 September 2024

Accepted: 29 April 2025

Published online: 13 May 2025

Check for updates

Wenbo Yuan[1], Tianyu Huang[1], Jianping Zhou[1], Man-Chung Tang[2], Dongdong Zhang[1] ✉ & Lian Duan[1,3] ✉

A suitable host material is pivotal for efficient and stable deep-blue phosphorescent organic light-emitting diodes (PhOLEDs). Here, we construct a deuterated exciplex-forming host with improved molecular stability and charge transport and firstly unveil an "external deuteration effect" on dopant, which reduces the shoulder emissions for slightly blue-shifted colours and also accelerates the radiative decay rates for improved photoluminescence efficiency. The corresponding deep-blue PhOLEDs based on two platinum complexes, PtON-TBBI and PtON-tb-DTB, achieve lower operational voltages and higher maximum external quantum efficiencies of 27.4/19.9% and power efficiency of 41.2/33.6 lm/W, respectively, compared to the hydrogen-based counterparts. Moreover, lifetimes of 370 and 557 h to reach 90% of the initial luminance of 1000 cd/m^2 with Commission Internationale de l'Eclairage coordinates of (0.148, 0.165) and (0.153, 0.213) are achieved, 1.6 and 1.4 times longer than the ones based on the non-deuterated hosts with even blue-shifted colours.

Organic light-emitting diodes (OLEDs) have been successfully commercialized as a new generation display. However, the OLEDs industry with a market of tens of billions of dollars still relies on inefficient deep-blue conventional fluorescent emitters[1–4]. Blue phosphorescent (PhOLEDs) and thermally activated delayed fluorescent OLEDs (TADF-OLEDs) have long been regarded as promising alternatives to blue fluorescent OLEDs, due to their theoretical capacity for achieving near-unity internal quantum efficiency (IQE)[5–7]. And recently significant advancements have been made in the development of stable luminescent blue materials[8–10], particularly platinum complexes following the initial work on PtON7-dtb[11]. However, the device stability is still limited by the lack of a suitable host material, of which the progress lags behind and is even more challenging considering not only the required higher energy levels than the dopant but also balanced and good charge transfer[4,12–15]. A breakthrough has recently been made by Sun and coworkers by developing a deep-blue exciplex-forming host (SiCzCz and SiTrzCz2)[10], based on which the deep-blue PhOLEDs achieved a long operational lifetime (LT_{70}, where LT_x indicates the time to reach x% of the initial luminance) of 1113 h at an initial luminance of 1000 cd m^{-2} with a y coordinate of 0.197, representing one of the longest lifetimes for deep-blue devices. Following this pioneer work, successive works on deep-blue OLEDs rely on SiCzCz: SiTrzCz2 to provide decent device lifetimes, evidencing the great potential of this system[8,11,16]. However, not only the stability but also the charge transport ability of SiCzCz: SiTrzCz2 still needs to be further improved as it always requires high device operational voltage. Improving the performances of SiCzCz: SiTrzCz2 therefore has been an exigent task, but facing formidable challenges.

Of particular note, deuteration has recently attracted much attention in the literature as an effective strategy for promoting device

[1]Key Laboratory of Organic Optoelectronics and Molecular Engineering of Ministry of Education, Department of Chemistry, Department of Chemistry, Tsinghua University, Beijing 100084, China. [2]Institute of Materials Research, Tsinghua Shenzhen International Graduate School, Tsinghua University, Shenzhen 518055, China. [3]Laboratory of Flexible Electronics Technology, Tsinghua University, Beijing 100084, China. ✉e-mail: ddzhang@mail.tsinghua.edu.cn; duanl@mail.tsinghua.edu.cn

stability due to the kinetic isotope effect[17–21], although such an effect can be traced back to 2010, when it was first observed in a green phosphorescent emitter[22]. Choi and Baik et al. recently realized a double enhancement on LT_{70} of blue PhOLEDs through deuterating the most vulnerable benzylic C-H bond in a blue Ir-phenylimidazole dopant to hamper the deactivation pathway involving C-H/D bond cleavage notably[23]. In this year, our group also explored the perdeuteration strategy for sky-blue TADF materials and obtained a three-fold longer device lifetime[24]. It was found that the isotopic substitution could suppress the high-frequency structural vibrations of TADF emitters, not only extending the operational lifespan of electroluminescent devices, but also inhibiting non-radiation energy loss for high efficiency. Besides emitting dopants, deuterated hosts have started to get studied also. Adachi et al. showed that a deuterated host material could realize an over two-time longer lifetime for green TADF device, due to the better morphological stability in the deuterated film[18]. Additionally, Tang and colleagues observed a correlation between the kinetic isotope effect of the photodegradation reactions and the enhancement in device lifetime through the simultaneous deuteration of the hole-transporting material and host material, realizing up to an eight-fold increase in LT_{90} of conventional fluorescent blue device[19]. Though the exact mechanism is still debating and complex, those preliminary works have evidenced the great potential of deuteration strategy.

Considering the highly needs on stable wide-energy-gap host, we here envisioned that the deuterated exciplex-forming host may further unlock the potential of deep-blue PhOLEDs. It is noticed that, however, all previous works studied deuterated single molecules and only focused on the optoelectronic property of deuterated materials themselves. This leaves us questions about how deuteration would affect the property of bimolecular exciplex-forming system and whether the property of the dopant would be influenced by the deuterated host. Bearing this in minds, we developed deuterated exciplex-forming host (*D*-SiCzCz: *D*-SiTrzCz2) following the classic protonated SiCzCz: SiTrzCz2 system, of which the underlying physics were thoroughly studied. It was found that, similar to the deuterated single molecule, the deuterated exciplex-forming host could also establish a better molecular intrinsic stability from the suppressed high-energy molecular vibrations and decreased chemical reactivity, and an improved charge transport ability due to the reduced molecular reorganization energy. More importantly, we unveiled an external deuteration effect from deuterated host to the dopant, which could provide a denser environment for phosphorescent dopant to reduce its shoulder emission intensity and also accelerate the radiative decay process for higher luminance efficiency and better stability. The corresponding deep-blue PhOLEDs using *D*-SiCzCz: *D*-SiTrzCz2 as host for Pt complexes simultaneously achieved not only lower operational voltages and higher device efficiencies, but also 1.4-1.6 times longer device lifetime with slightly bluer electroluminescence colour compared with the protonated counterparts. Our work not only provides a better host for highly efficient and stable deep-blue devices, but also firstly demonstrated new scientific findings about the external deuteration effect, deepening our understanding of the kinetic isotope effect of deuteration strategy.

Results

Molecular synthesis and computational results

The molecular structures of *D*-SiCzCz and *D*-SiTrzCz2 were provided in Fig. 1a. It needs to point out that only the carbazole units of both molecules were deuterated. On one hand, it is believed that the hydrogen atoms on the carbazole units were more chemically active and functional. And the tetraphenylsilane segment is believed to only partially participate into the electronic distribution of the molecule owing to its nonconjugation structure. On the other hand, the deuterated carbazole is commercially available, which would greatly reduce the cost for practical applications compared with the perdeuterated molecules considering the synthesis difficulty. The synthetic routes of the two compounds were illustrated in Supplementary Fig. 1. For *D*-SiCzCz, in order to realize Buchwald-Hartwig coupling reaction, the active site of 3-bromo-9*H*-carbazole-1,2,4,5,6,7,8-d_7 was protected by *t*-butyloxycarbonyl unit. The protective group was removed under acidic condition to ensure subsequent coupling with tetraphenylsilicon moiety. *D*-SiTrzCz2 were synthesized through nucleophilic substitution and Buchwald-Hartwig coupling reaction according to literature[10]. The chemical structure of the two compounds were confirmed by ^{1}H NMR, ^{13}C NMR and MALDI-TOF mass spectrometry (Supplementary Fig. 2–10). Thermal properties of *D*-SiCzCz and *D*-SiTrzCz2 were also examined by thermogravimetric analysis (TGA) and differential scanning calorimetry (DSC) under nitrogen atmosphere (Supplementary Fig. 11). The decomposition temperatures (corresponding to 5% weight loss) are 380 and 432 °C, respectively, indicating that both materials are sufficiently thermally stable. The glass transition temperatures were observed at 117 and 121 °C for *D*-SiCzCz and *D*-SiTrzCz2 on the second heating cycle. The absence of melting point and crystallization temperature may be attributed to the strong amorphous character, which would be beneficial for stable device operation even at high temperatures.

To gain further insight into the nature of the deuterated and non-deuterated compounds, the density functional theory (DFT) calculations were performed (Supplementary Fig. 12). The highest occupied molecular orbitals (HOMOs) of electron donors were predominantly localized on the bi-carbazoles, while the lowest unoccupied molecular orbitals (LUMOs) of electron acceptors were mainly distributed on the triazine and adjacent phenyl moiety. This demonstrated that the deuteration had no direct effect on the orbital distribution owing to the Born-Oppenheimer approximation. The HOMO and LUMO distributions in the ionic state were also presented in order to facilitate intuitive understanding of the chemical activity. As illustrated in Supplementary Fig. 13 and Supplementary Fig. 14, the HOMOs of the electron donors were primarily distributed on the carbazoles, indicating that the carbazole moieties participate in the charge transfer process in cationic state. Conversely, in anionic state, neither the HOMOs nor the LUMOs of the electron acceptors were distributed on the carbazole moieties. This verified that the carbazoles in acceptors serve solely as spatial functional groups and do not contribute to the interaction of electron orbitals, which becomes one of the reasons for the subsequent difference in performance.

To find out the deuteration effect on the molecular vibrations, Fourier transform infrared (FT-IR) spectra were simulated in Fig. 1b and c. As anticipated, the distinctive band attributed to the C-H stretching mode at 3203 cm^{-1} gradually decreased and a novel absorption peak for the C-D stretching mode at 2376 cm^{-1} emerged in the spectra of *D*-SiCzCz and *D*-SiTrzCz2. Similar variations were also observed in the experimental infrared spectra as shown in Supplementary Fig. 15, where the high energy absorption bands at 3046 and 3047 cm^{-1} were significantly suppressed while new absorption bands at 2264 and 2266 cm^{-1} exhibited pronounced distinctions, substantiating the reduction of molecular energy subsequent to deuteration. Considering that the unchanged molecular skeleton and the vibrational degrees of freedom, these changes in FT-IR absorption intensity can be attributed to the suppression of high frequency vibrations after deuteration. Furthermore, the zero-point energy (ZPE) values were also calculated before and after deuteration[25], with a notable reduction from 1782.77 to 1653.37 KJ/mol for donors and from 1904.84 to 1766.03 KJ/mol for acceptors. The differences are mainly observed in the C-D bonds, which exhibited lower frequency vibrations, while the vibrations of the C-C and C-N bonds remains at a base value (Fig. 1d and e). The combination of ZPE values and FT-IR results demonstrated that deuterated materials should exhibit a relatively lower population at high vibrational energy levels, which is advantageous for the intrinsic

https://doi.org/10.1038/s41467-025-59583-8

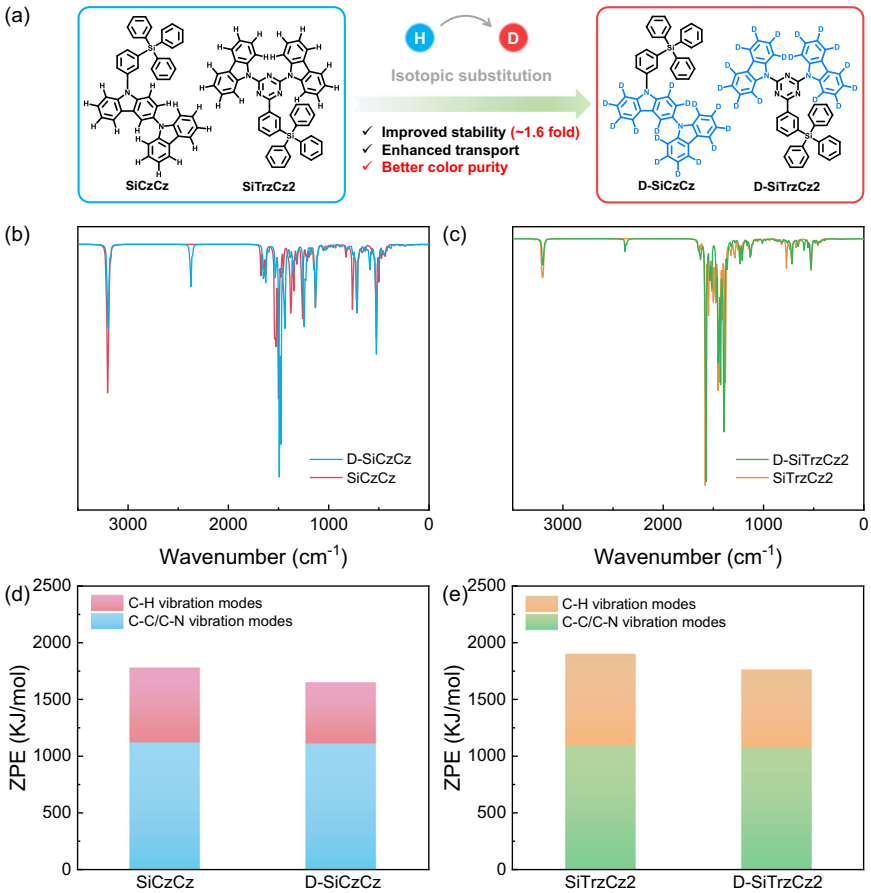

Fig. 1 | Schematic illustration of molecular design strategy. a Diagram of the molecular design strategy and chemical structures of the target and reference molecules. The simulated Fourier transform infrared (FT-IR) spectra of **b** *D*-SiCzCz and SiCzCz, **c** *D*-SiTrzCz2 and SiTrzCz2. The contributions of individual vibration modes to the entire molecular zero-point energies (ZPEs) of **d** SiCzCz and *D*-SiCzCz, **e** SiTrzCz2 and *D*-SiTrzCz2.

stability of the host materials under excited states. In order to have a more intuitive understanding on the effect of deuteration on structural stability[26–28], we also calculated the bond dissociation energies (BDEs) in positive, negative and neutral states for electron donors and acceptors, respectively (Supplementary Table 1). The BDE values of the C-D bonds are significantly higher than those of the C-H bonds in both the neutral and ionic states, manifesting the isotope effect on the intrinsic structural stability. The enhancement of bond energy in negative state (BDE(-)) can effectively inhibit the reactivity of carbazoles at 3- and 6-position, thus providing a rigid environment to significantly reduce destructive deactivation of the excited states. It is therefore anticipated that the elevated degree of deuteration on both electron donors and acceptors can exert a more pronounced effect on the stability of exciplexes.

Photophysical and electronic properties

The ultraviolet-visible (UV-vis) absorption and photoluminescence (PL) spectra at both room temperature and 77 K in dilute toluene solution are shown in Supplementary Fig. 16. *D*-SiCzCz and *D*-SiTrzCz2 exhibited intense absorption bands between 300 and 360 nm, which were assigned to the π-π^* transition absorption. The deuterated donor and acceptor featured broad structureless emission bands with peak values at 372 and 431 nm, as shown in Supplementary Fig. 17. The emission curves exhibited a narrowing of ~1 nm and a blue shift of ~1 nm in comparison with the protonated counterparts, which may be attributed to the large Franck-Condon integral of the deuterated compounds with more compact vibrational energy alignment[24]. The singlet and triplet energies of *D*-SiCzCz and *D*-SiTrzCz2 estimated from the onset point of the fluorescence and phosphorescence spectra were 3.51/3.09 and 3.29/3.06 eV, respectively. These values were similar to those of the non-deuterated compounds. Their absorption and emission curves in film state also exhibited no significant difference with contrast molecules (Supplementary Fig. 18 and Supplementary Table 2). As shown in Fig. 2a, the emission of *D*-SiCzCz: *D*-SiTrzCz2 and SiCzCz: SiTrzCz2 mixtures were both located at 466 nm, exhibiting an obvious red-shifted trend in contrast to their respective constituent components (*D*-SiCzCz: 377 nm, *D*-SiTrzCz2: 427 nm, SiCzCz: 387 nm and SiTrzCz2: 428 nm), indicating their emissions should be from the exciplexes. Such exciplex formation could also be confirmed by analysing the transient PL decay of the mixtures, as shown in Supplementary Fig. 19. It was observed that the deuterated exciplex exhibited a prolonged lifetime with a delayed component of 648.8 ns (Supplementary Table 2), which is considerably longer than the nanosecond lifetime of the individual components. Meanwhile, the triplet energies of the exciplexes were measured to be 2.95 and 2.90 eV for deuterated and non-deuterated mixtures, respectively (Supplementary Fig. 20). These results suggest that deuteration has a negligible effect on the energy levels involved in the radiative processes. To investigate the effect of deuteration on the intrinsic photostability of the exciplex-forming host materials, we performed PL stability test of the protonated and deuterated mixtures in vacuum-evaporated films (with thickness of 100 nm) by continuous ultraviolet irradiation with a peak wavelength of 360 nm (Supplementary Fig. 21 and 22). Apparently, the shape of the emission bands remains unchanged, but the proportion generally declined to a lesser extent with the extension of the exposure time. The relative intensity decreased from 100% to 93% and 86% for *D*-SiCzCz: *D*-SiTrzCz2 and SiCzCz:

https://doi.org/10.1038/s41467-025-59583-8

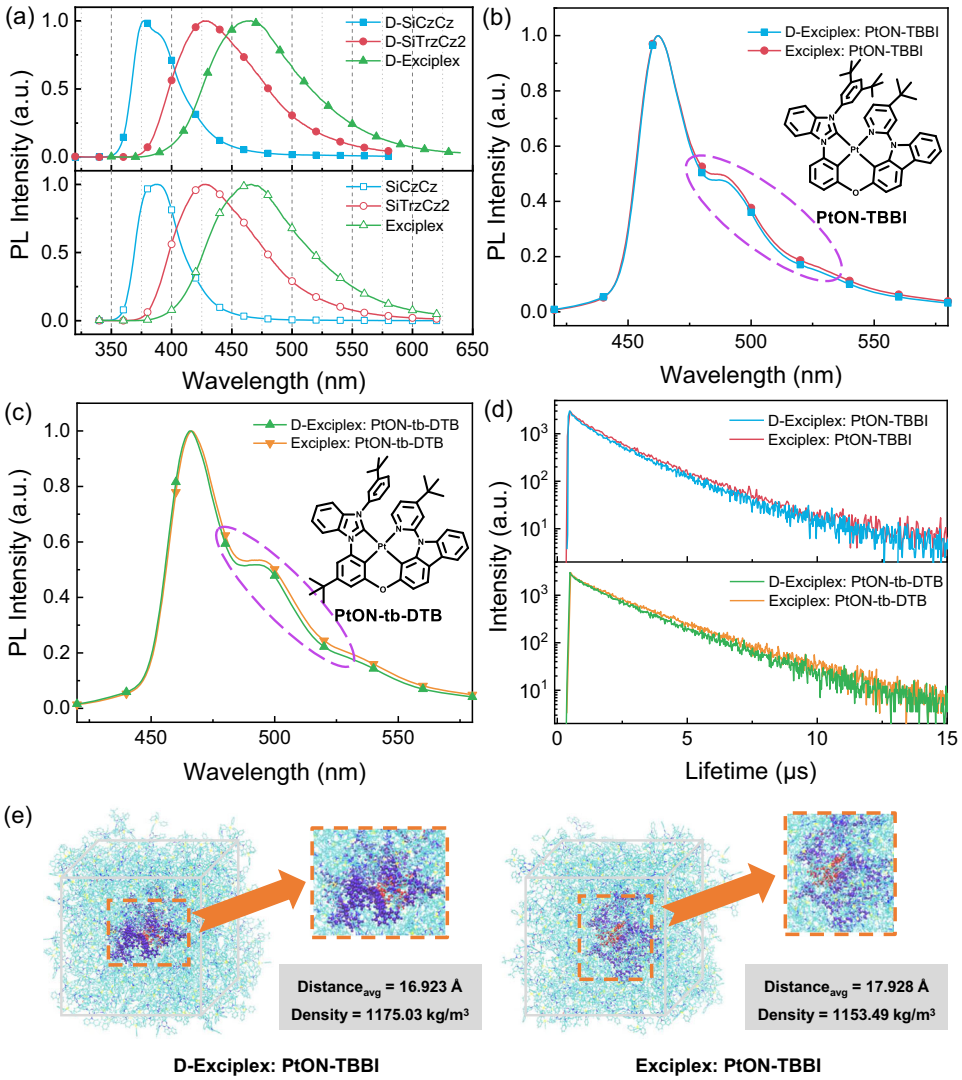

Fig. 2 | Photophysical properties of the deuterated and non-deuterated exciplexes and their related doping films. a PL spectra overlap of *D*-SiCzCz/SiCzCz, *D*-SiTrzCz2/SiTrzCz2 and the relevant exciplexes in film state. PL spectra of deuterated and non-deuterated exciplexes doped with **b** 10 wt% PtON-TBBI or **c** PtON-tb-DTB in film state. **d** Transient decay curves of deuterated and non-deuterated exciplexes doped with 10 wt% PtON-TBBI (up) or PtON-tb-DTB (down) in film state. **e** Molecular dynamic (MD) simulation results of the deuterated and non-deuterated exciplexes doped with 10 wt% PtON-TBBI (donor: acceptor = 65: 35, red structure: one selected PtON-TBBI molecule, purple structures: surrounded donors and acceptors). Distance$_{avg}$: the average distance between the selected PtON-TBBI molecule and surrounded donors and acceptors. Density: the density of all the mixtures in the entire box.

SiTrzCz2 mixtures, indicating a positive deuteration effect on the photostability of the host materials[19].

To find out the deuterated host influence on the photophysical properties of the dopant, we fabricated the doped films using 10 wt% PtON-TBBI as the emitter, where PtON-TBBI stands for Platinum(II) [2-[3-[3-[3,5-bis(1,1-dimethylethyl)phenyl]−1H-benzimidazol-1-yl-κC2] phenoxy-κC2]−9-[4-(1,1-dimethylethyl)−2pyridinyl-κN]−9H-carbazolato(4-)-κC1]. This dopant has demonstrated to be a stable deep-blue phosphorescent emitter with narrowband emission[10]. The PL spectra of the doped films are shown in Fig. 2b. Interestingly, though their same maximum peak values at 462 nm, a relatively smaller full-width at half-maximum (FWHM) of 27 nm was observed from the deuterated host, in comparison to the value of 29 nm from the non-deuterated one. This result originates from the reduction of those shoulder peaks between 475 and 575 nm. As those shoulder peaks usually come from the large-energy vibration levels of the dopant, those results suggest that deuterated hosts could help to suppress the high frequency vibrations of the dopant[10,11]. This can be further reflected by a slightly enhanced PLQY of 97% in deuterated host with a relatively shorter radiative decay lifetime of 2.35 μs (Table 1 and Fig. 2d), which were 94% and 2.42 μs in non-deuterated host, respectively. The lowered vibrations could suppress the vibronic coupling between the high vibration levels of the ground states and the low vibration levels of the excited states, thus favouring to suppress non-radiative decay for a high PLQY. The shorter decay lifetime was consequently attributed to the elevated rate constants of radiation (k_r), which were calculated to be $4.13 \times 10^7\,s^{-1}$ for deuterated mixtures, exhibiting a notable increase in comparison to protonated mixtures ($3.88 \times 10^7\,s^{-1}$). To verify the universality of the influence on the photophysical properties, further measurements were conducted on the PL spectra and transient decay curves of PtON-tb-DTB doped films (Fig. 2c and d). The mixture based on deuterated exciplex-forming host exhibited a comparable reduction in the intensity of the shoulder peaks, with an even greater magnitude due to the enhanced flexibility compared to that observed in PtON-TBBI. Moreover, the deuterated mixture showed similarly shorter decay lifetime, higher PLQY and enhanced k_r, thereby substantiating the favourable impact on accelerating radiation (Table 1). To explain those differences, we conducted a molecular dynamic (MD)

Table 1 | Summary of the photophysical properties of the deuterated and nondeuterated exciplexes

Compounds	λ_{em}[a] [nm]	λ_{ex}[b] [nm]	E_T[c] [eV]	τ_d[d] [μs]	Φ_{PL}[d] [%]	k_r[e] [$\times10^7 s^{-1}$]
D-SiCzCz	377	466	2.95	2.35/ 2.27	97/92	4.13/4.05
D-SiTrzCz2	427					
SiCzCz	387	466	2.90	2.42/ 2.50	94/87	3.88/3.48
SiTrzCz2	428					

[a]PL emission measured in pristine film at room temperature.
[b]Exciplex emission measured in vacuum-evaporated films.
[c]Triplet energy measured through low temperature (77 K) phosphorescence spectra in exciplex-forming films.
[d]Transient decay and PLQY measured in 10 wt% PtON-TBBI/PtON-tb-DTB doped exciplex-forming films.
[e]Rate constants of radiation calculated using $k_r = \Phi_{PL}/\tau_d$.

simulation to ascertain the detailed information of the stacking mode of the host materials and PtON-TBBI. As depicted in Fig. 2e, the average distances between the randomly selected PtON-TBBI molecule and adjacent donors and acceptors were reduced from 17.928 Å for non-deuterated mixture to 16.923 Å for deuterated mixture, accompanied by an increased density from 1153.49 to 1175.03 kg/m^3. Although the increased density may mainly be attributed to the heavier deuterium substitution, the enlarged compactness surrounding the phosphorescent dopants still provides a rigid and compact environment, thereby inversely suppressing the structural vibrations in deuterated exciplex-forming host. In this way, we firstly unveiled an external deuteration effect on dopant, which could expect a higher colour purity and a higher PLQY with faster radiative decay from the same dopant in deuterated hosts, and this would greatly deepen our understanding of the isotope effect.

To figure out the effect of isotope substitution on charge transport characteristics of single donor/acceptor and relevant exciplex-forming host materials, hole-only and electron-only devices (HODs and EODs) were fabricated. The device configurations of HOD and EOD were indium tin oxide (ITO)/1,4,5,8,9,11-hexaazatriphenylenehexacabonitrile (HATCN, 5 nm)/*N,N'*-bis-(1-naphthalenyl)-*N,N'*-bis-phenyl-(1,1'-biphenyl) −4,4'-diamine (NPB, 30 nm)/Host (50 nm)/NPB (30 nm)/MoO_3 (5 nm)/Al (150 nm) and ITO/Cs_2CO_3 (1 nm)/4,7-Diphenyl-1,10-phenanthroline (Bphen, 5 nm)/9,10-Bis(6-phenylpyridin-3-yl) anthracene (DPPyA, 30 nm)/Host (50 nm)/DPPyA (30 nm)/LiF (0.7 nm)/Al (150 nm), respectively. In the HODs and EODs for single donor and acceptor, *D*-SiCzCz and *D*-SiTrzCz2 exhibited markedly higher current density than that of the non-deuterated counterparts at the same voltage, as illustrated in Supplementary Fig. 23. In the case of the exciplexes, the increase in current density is still clearly discernible. At a voltage of 11 V, the current density of the HODs based on deuterated exciplexes was approaching the detection limit (420 mA cm^{-2}), whereas the value of the non-deuterated one remained below 100 mA cm^{-2} (Fig. 3a). On the other hand, the current density of EOD was also found to have reached the detection limit at approximately 9 V, which is considerably superior to that of the non-deuterated counterparts (Fig. 3b). These results demonstrated that the deuteration has a considerable impact on the carrier transport character of the exciplex-forming hosts, with the enhancement of hole transport in donors being particularly notable.

In organic semiconductors, charge transfer is through a hopping mode, which can be described by the Marcus electron transfer theory:

$$k_{et} = \left(\frac{4\pi^2}{h}\right) J^2 (4\pi T\lambda)^{-\frac{1}{2}} e^{-\frac{\lambda}{4kT}} \quad (1)$$

where h is Plank constant, k is Boltzmann constant, T is temperature, λ is reorganization energy, and J is charge transfer integral between two molecules (Fig. 3c)[29–34]. At a given temperature, the electron transfer rate (k_{et}) is determined by J and λ. Since the more compact molecular stacking after deuteration, the charge transfer integral (J) for deuterated exciplexes can be slightly higher and thus achieving better charge transport. Besides, we also analysed the reorganization energy (λ) of those molecules before and after deuteration. As depicted in Fig. 3d, the λ values of electron donors expressively reduced from 0.775 eV for SiCzCz to 0.655 eV for *D*-SiCzCz, while mildly decreased for electron acceptors from 0.655 eV for SiTrzCz2 to 0.628 eV for *D*-SiTrzCz2 (Supplementary Fig. 24 and 25). The discrepancy in the extent of reduction may be attributed to the influence of the site of deuterium substitution. In the case of the donor component, the deuterium substitutions take place on the carbazoles, which are directly implicated in charge transfer, and thus the reduction of reorganization energy for *D*-SiCzCz is considerable. Conversely, in the acceptor component, the carbazoles are not directly involved in charge transfer, therefore, the alteration in reorganization energy for *D*-SiTrzCz2 is relatively modest. This also explained why donors showed a more significant enhancement on charge transport than acceptors aforementioned. Overall, an increase in J and a decrease in λ together enhance the charge transport capability of those materials, finally resulting in higher current densities in electron only devices.

The interaction between the triplet excitons of the dopants and the polarons of the hosts represents a significant factor contributing to the stability of blue-emitting devices. Therefore, it is essential to monitor the stability of the polarons in the exciplex-forming host materials before and after deuteration. Electrical-aging measurements in single carrier devices were conducted under a constant current of 1.2 mA to assess the stability of single donor/acceptor and exciplex-forming hosts. When subjected to the same current density, both deuterated compounds and their corresponding exciplexes exhibited lower voltage throughout the entire test. In the devices based on single donor, the voltage increasement was observed to be 0.51 and 1.05 V for *D*-SiCzCz and SiCzCz, respectively (Supplementary Fig. 26). In comparison, the corresponding increasement for *D*-SiTrzCz2 and SiTrzCz2 were significantly higher (0.95 and 2.28 V), manifesting that the relatively poor stability for the polarons in electron acceptors. A similar statement has been reported by Choi and Kim, who determined that the suppression of electron-induced degradation played a pivotal role in enhancing operational stability[35]. In the exciplex-based devices, compared to the voltage increase in HODs, the growth was more pronounced in EODs (Supplementary Fig. 27). Taking advantage of the isotope effect, the voltage increase was reduced from 1.07 V for non-deuterated exciplex to 0.49 V for deuterated exciplex, indicating an effective route to inhibit electron-induced degradation processes. Furthermore, the photoelectrical aging experiments were also carried out by recording the driving voltage increase under the operation at a current density of 10 mA cm^{-2} and a 355 nm UV light irradiation with a power of 10 mW. As depicted in Fig. 3e and f, both the hole-only and electron-only devices based on deuterated exciplexes showed smaller change within 1.6 V, while the devices based on protonated exciplexes showed distinctly large change of over 2 V. These outcomes suggest an objective enhancement of both the triplet exciton and polaron stability for exciplex-forming host materials.

Device characterization and performance

The EL performance of the deuterated exciplex-forming hosts was evaluated by fabricating devices with the following structure: ITO/HATCN (5 nm)/NPB (30 nm)/Exciplex donor (10 nm)/Host: PtON-TBBI or PtON-tb-DTB (30 nm, 65:35:10 wt%)/Exciplex acceptor (10 nm)/DPPyA: Liq (40 nm, 50:50 wt%)/LiF (0.7 nm)/Al (150 nm). It is noted that the electron-donating and accepting parts of exciplexes are employed not only as host materials, but also as electron- and hole-blocking materials. The energy level diagram and device configuration are shown in Fig. 4a. The HOMO and LUMO energies of the deuterated components were measured by cyclic voltammetry in dichloromethane and tetrahydrofuran solution (Supplementary Fig. 28).

https://doi.org/10.1038/s41467-025-59583-8

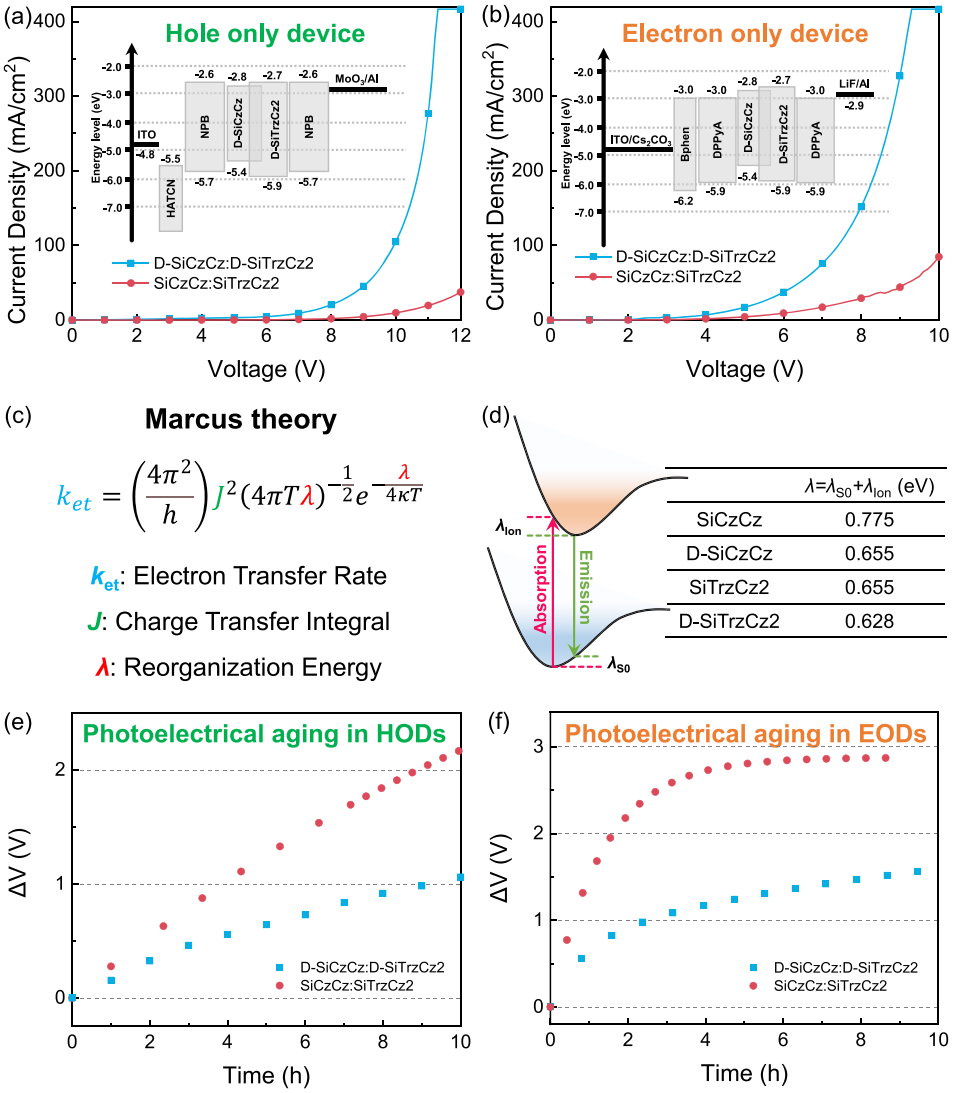

	$\lambda=\lambda_{S0}+\lambda_{Ion}$ (eV)
SiCzCz	0.775
D-SiCzCz	0.655
SiTrzCz2	0.655
D-SiTrzCz2	0.628

Fig. 3 | Single-carrier device performance and reorganization energy analysis. Current density-voltage characteristics of **a** hole-only devices (HODs) and **b** electron-only devices (EODs) for deuterated and non-deuterated mixtures (The inset shows the device structures of HODs and EODs). **c** Marcus electron transfer theory. **d** Reorganization energies (λ) of the deuterated and non-deuterated compounds. Voltage rise plots in photoelectrical aging of **e** HODs and **f** EODs based on protonated and deuterated mixtures.

As depicted in Fig. 4b, when subjected to the same driving voltage, the current density of device A is obviously higher than that of device B, allowing it to achieve the detection limit of photocurrent sooner than device B. Meanwhile, the driving voltage of device A is relatively lower at any luminance level between the turn-on state and their maximum luminance of 25080 and 17870 cd m^{-2}. The turn-on voltage and operational voltage at 1000, 5000, 10,000 cd m^{-2} were 2.5, 4.2, 5.7 and 6.6 V for device A, respectively, while the corresponding values are 2.6, 4.5, 6.1 and 7.2 V for device B. These results are believed to be attributed to the superior hole- and electron-transporting capabilities of *D*-SiCzCz, *D*-SiTrzCz2 and the corresponding exciplexes, as demonstrated above. The EL spectra of both device A and B exhibited narrow emission bands with peak value of 461 nm and FWHM of 24 and 26 nm, respectively, indicating highly efficient energy transfer from exciplex-forming hosts to PtON-TBBI emitter (Fig. 4c). It is worth noting that the spectral shoulder peaks of the device based on deuterated exciplex are lower, which is consistent with the photoluminescence spectra of the doped film shown in Fig. 2b. As a consequence, the CIE coordinates of device A is found to be bluer with smaller CIE$_y$ of 0.165, suggesting a positive influence for deep-blue exciplex-forming hosts (Table 2). In the meantime, the devices utilizing PtON-tb-DTB as phosphorescent dopant were fabricated to gain deeper insight into its impact on the EL spectra. As depicted in Fig. 4b, both device C and D showed similar trend with device A and B, exhibiting distinctly lower driving voltages in device C, which was based on the deuterated exciplex-forming host. Significantly, we have also observed a reduction in the spectral shoulder peaks within PtON-tb-DTB-based device C, compared to device D (Fig. 4d), coincident with a blue shift in the CIE coordinates from (0.153, 0.213) to (0.156, 0.217). This outcome is congruent with the EL performance of the aforementioned PtON-TBBI-based device A and B, but varies to a lesser extent than the PL spectra of the doped films. Collectively, these findings validate that the spectral narrowing is a consequence of the interaction between the deuterated host matrixes and the phosphorescent dopants, and the microcavity effect inherent to the device architecture may even weaken the external deuteration effect to some extent.

The external quantum efficiency (EQE) and power efficiency (PE) *versus* luminance curves are shown in Fig. 4e. As illustrated, the maximum PE/EQE values of 41.2 lm W^{-1}/27.4% were achieved for device A, which were slightly higher than those of contrast device B (36.9 lm W^{-1}/27.1%). Notably, the EQE of device A was maintained at a high level of

https://doi.org/10.1038/s41467-025-59583-8

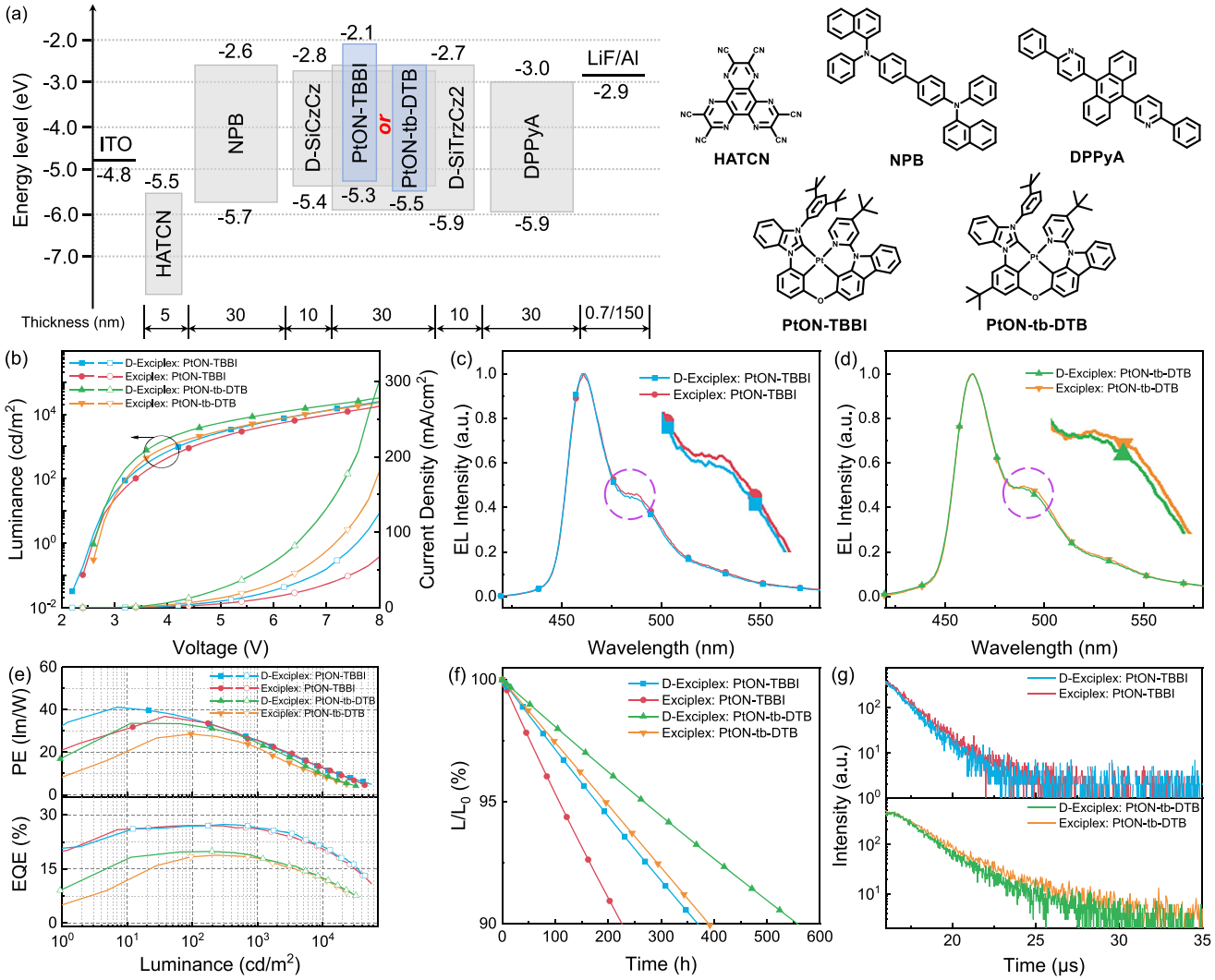

Fig. 4 | Optimized electroluminescent properties of phosphorescent OLEDs. **a** Device structure, energy level diagrams and molecular structures of the materials. **b** Luminance-voltage-current density (*L-V-J*) characteristics (the solid symbol represents luminance and the hollow symbol represents current density). Normalized EL spectra of the devices based on **c** PtON-TBBI and **d** PtON-tb-DTB. **e** Power efficiency (PE) and external quantum efficiency (EQE) *versus* luminance curves of the devices based on PtON-TBBI and PtON-tb-DTB. **f** Operational lifetime curves at initial luminance of 1000 cd m^{-2}. **g** Transient EL decay curves of the devices based on PtON-TBBI and PtON-tb-DTB.

Table 2 | Summary of the EL performance

	Hosts	Dopants	$V_{on/1000/5000/10000}$[a] [V]	L_{max}[b] [cd/m^2]	$PE_{max/1000/5000}$[c] [lm/W]	$EQE_{max/1000/5000}$[d] [%]	λ_{EL}[e] [nm]	FWHM[f] [nm]	CIE (x,y)[g]	LT_{90}[h] [h]
A	D-Exciplex	PtON-TBBI	2.5/4.2/5.7/6.6	25080	41.2/25.9/16.7	27.4/26.4/23.7	461	24	(0.148,0.165)	370
B	Exciplex		2.6/4.5/6.1/7.2	17870	36.9/25.7/16.9	27.1/26.2/22.7	461	26	(0.149,0.172)	226
C	D-Exciplex	PtON-tb-DTB	2.6/3.7/4.9/5.9	32110	33.6/24.2/14.3	19.9/18.3/14.8	464	28	(0.153,0.213)	557
D	Exciplex		2.7/4.0/5.6/6.6	23240	28.5/22.0/12.3	18.9/18.0/14.3	464	28	(0.156,0.217)	390

[a]Turn-on voltage at 1 cd m^{-2} and operational voltages at 1000/5000/10,000 cd m^{-2}.
[b]Maximum luminance.
[c]Maximum power efficiency and corresponding values at 1000/5000 cd m^{-2}.
[d]Maximum external quantum efficiency and corresponding values at 1000/5000 cd m^{-2}.
[e]Peak value of EL spectra.
[f]Full-widths at half-maximum.
[g]Commission Internationale de L'Eclairage (CIE) coordinates.
[h]Time to 90% of the initial luminance.

26.4 and 23.7% at a luminance of 1000 and 5000 cd m^{-2}, respectively. This corresponds to an efficiency roll-off of only 3.6 and 13.5%, indicating that the device with deuterated exciplex-forming host materials exhibited superior EL stability at high brightness. Similarly, device C exhibited higher efficiencies than device D, with a maximum EQE of 19.9% and a maximum PE of 33.6 lm W^{-1}. At luminance of 1000 and 5000 cd m^{-2}, the EQEs were preserved at 18.3 and 14.8%, respectively, along with PE values of 24.2 and 14.3 lm W^{-1}. The device lifetime was then evaluated under initial luminance of 1000 cd m^{-2} (Fig. 4f). Impressively long LT_{90} values of 370 h was observed for device A,

which is ~1.6-fold that of the device B based on non-deuterated hosts (~226 h). By employing PtON-tb-DTB with prolonged lifetime as the phosphorescent dopant, the stability of deep-blue OLEDs was markedly improved. Device C based on deuterated exciplex-forming host exhibited an extended operational lifespan of 557 h, which is approximately 1.4-fold greater than that of device D (390 h) using non-deuterated counterparts. To the best of our knowledge, device A and C are one of the most stable deep-blue devices with $CIE_y < 0.22$ as summarized in Supplementary Fig. 29 and Supplementary Table 3. The notable enhancement in device stability naturally originates from the adoption of deuterated exciplex-forming host, which possesses not only better intrinsic stability but also improved charge transport ability. Additionally, the electroluminescence decay behaviours of all the devices were also measured as shown in Fig. 4g. Clearly, similar to the PL results, PtON-TBBI and PtON-tb-DTB in deuterated host exhibited a distinctly faster radiative decay process, thus favouring to suppress the triplet-related annihilations for extended device lifetime. Of particularly note, device A and C with deuterated host achieves not only smaller y-colour coordinate, but also significantly prolonged device lifetime. This is contrary to conventional wisdom that a bluer emission would always deteriorate the device stability[36–38]. As in this case, the bluer colour was achieved not by blue-shift the emission maximum but through reducing the emission shoulder for better colour purity. It should also be noted that the reduced shoulders could eliminate the energy loss in top-emitting devices with microcavity and thus enhance device efficiency in terms of blue index (BI), defined as the ratio of current efficiency to CIE_y coordinate.

Discussion

In summary, we developed a deuterated exciplex-forming host (*D*-SiCzCz: *D*-SiTrzCz2) for deep-blue phosphorescent OLEDs, derived from the previous reported promising SiCzCz: SiTrzCz2 exciplex-system. Besides the improved carrier transporting capabilities and device stability, we firstly unveiled an external deuteration effect of exciplex-forming host on the dopants. Deuteration was found to enlarge the compactness of the host and thus provide a rigid environment to suppress the dopant deformation, consequently decreasing the shoulder emission intensity of the dopants for bluer colour and accelerating the radiative decay process for a shorter lifetime of excited states meanwhile. The corresponding PhOLEDs based on PtON-TBBI and PtON-tb-DTB displayed dramatically longer lifespan of 370 and 557 h at an initial luminance of 1000 cd m^{-2}, which are 1.6 and 1.4 times longer than that of the control device. The EL spectra exhibited reductions in the intensity of the shoulder peaks with bluer CIE coordinates of (0.148, 0.165) and (0.153, 0.213), respectively. All those performances represent one of the best results among deep-blue devices. Given the lack of sufficient attention on the deuteration of host materials, our work offered a valuable contribution, elucidating the impact of deuterated exciplexes and facilitating the advancement of stable and efficient blue OLEDs.

Methods

General information

All chemical reagents for synthetic procedures were procured from Shanghai Bide Medical Technology Co. Ltd., while materials for device fabrication were supplied by Jilin Optical and Electronic Materials Co. Ltd. All materials were utilized as received without additional purification. Nuclear magnetic resonance (NMR) spectra (^{1}H: 600 MHz; ^{13}C: 151 MHz) were acquired on a JEOL JNM-ECS600 spectrometer using deuterated dichloromethane as solvent with tetramethylsilane (TMS) as internal reference. Matrix-assisted laser desorption/ionization time-of-flight mass spectrometry (MALDI-TOF-MS) analysis was conducted on a Shimadzu AXIMA Performance system in positive ion mode. Thermogravimetric analysis (TGA) measurements were performed under nitrogen atmosphere using a Q600 SDT analyzer with a heating rate of 10 °C min^{-1}.

Computational methods

Quantum chemical calculations were executed via Gaussian 16 and ORCA software packages under gas-phase conditions[39–44]. Ground-state geometries were optimized at the B3LYP/6-31 G(d) level, with subsequent vibrational frequency analysis incorporating standard scaling factors[45]. Single-point energy calculations employed the ωB97X-2-D3/def2-TZVP method implemented in ORCA 5.0. Zero-point energy (ZPE) corrections were computed using the Shermo program[25]. Bond dissociation energies (BDEs) for polaronic and neutral states were determined through frequency analyses of molecular fragments. Molecular dynamics (MD) simulations utilized GROMACS 2018.4[46,47], constructing a tricomponent system containing 195 donors, 105 acceptors, and 30 PtON-TBBI molecules within a cubic periodic boundary cell to model exciplex formation and doping processes.

Photophysical characterization

Solution-phase measurements employed samples diluted to 1×10^{-5} M concentration. Thin-film specimens were prepared via thermal evaporation on quartz substrates (deposition rate: 1-2 Å s^{-1}, base pressure: <10^{-5} Torr). UV-vis absorption spectra and photoluminescence (PL) profiles were recorded using a Shimadzu UV-2600 spectrophotometer and Horiba FluoroMax-4P fluorometer at 298 K and 77 K. Absolute photoluminescence quantum yields (PLQYs) were determined via Hamamatsu C9920-03G integrating sphere system under nitrogen-purged (solutions) or ambient (films) conditions. Time-resolved PL measurements were conducted on an Edinburgh FLS1000 fluorescence spectrometer.

Electrochemical analysis

Cyclic voltammetry measurements employed a CHI 660E electrochemical workstation configured with a Pt working electrode, Pt counter electrode, and Ag/Ag^+ reference electrode. Experiments were conducted in anhydrous dichloromethane and tetrahydrofuran containing 0.1 M TBAPF6 electrolyte at 100 mV s^{-1} scan rate.

Optoelectronic device fabrication

OLEDs were fabricated via thermal evaporation on pre-patterned ITO-glass substrates. All organic materials underwent vacuum gradient sublimation prior to deposition. Multilayer architectures were constructed in a high-vacuum chamber (<10^{-6} Torr) with controlled deposition rates (0.1–0.2 nm s^{-1} for organic layers). Doped layers were achieved through co-evaporation from independent crucibles with calibrated rate monitoring. Current-voltage-luminance characteristics and external quantum efficiency (EQE) were simultaneously recorded using a Keithley 2400 source meter coupled with a Hamamatsu C9920-12 EQE measurement system equipped with a PMA-12 multichannel analyzer (spectral range: 200–1100 nm). The EL decay behaviours were detected via an Edinburgh FLS1000 transient spectrometer with the device being excited by a short-pulse generated by an Agilent 8114 A. The device operational lifetimes were measured using an OLED aging lifetime tester (ZJZCL-1, Shanghai University). Measurements were taken in a standard laboratory with a RT around 20–30 °C and a humidity of 20-40%.

Data availability

The data supporting the findings of this study are available within the paper and the Supplementary Information. Source data are provided with this paper.

References

1. Zhang, Q. S. et al. Efficient blue organic light-emitting diodes employing thermally activated delayed fluorescence. *Nat. Photonics* **8**, 326–332 (2014).
2. Im, Y. et al. Recent progress in high-efficiency blue-light-emitting materials for organic light-emitting diodes. *Adv. Funct. Mater.* **27**, 1603007 (2017).

3. Cai, X. Y. & Su, S. J. Marching toward highly efficient, pure-blue, and stable thermally activated delayed fluorescent organic light-emitting diodes. *Adv. Funct. Mater.* **28**, 1802558 (2018).
4. Wang, Y., Yun, J. H., Wang, L. & Lee, J. Y. High triplet energy hosts for blue organic light-emitting diodes. *Adv. Funct. Mater.* **31**, 2008332 (2021).
5. Holmes, R., Forrest, S., Tung, Y.-J., Kwong, R. & Brown, J. Blue organic electrophosphorescence using exothermic host–guest energy transfer. *Appl. Phys. Lett.* **82**, 2422–2424 (2003).
6. Hopkinson, M. N., Richter, C., Schedler, M. & Glorius, F. An overview of N-heterocyclic carbenes. *Nature* **510**, 485–496 (2014).
7. Cao, L., Klimes, K., Ji, Y., Fleetham, T. & Li, J. Efficient and stable organic light-emitting devices employing phosphorescent molecular aggregates. *Nat. Photonics* **15**, 230–237 (2021).
8. Lee, H. et al. Superbly efficient and stable ultrapure blue phosphorescent organic light-emitting diodes with tetradentate Pt(II) complex with vibration suppression effect. *Adv. Mater.* **36**, 2409394 (2024).
9. Jung, Y. H. et al. Modified t-butyl in tetradentate platinum (II) complexes enables exceptional lifetime for blue-phosphorescent organic light-emitting diodes. *Nat. Commun.* **15**, 2977 (2024).
10. Sun, J. et al. Exceptionally stable blue phosphorescent organic light-emitting diodes. *Nat. Photonics* **16**, 212–218 (2022).
11. Li, G., Ameri, L., Dorame, B., Zhu, Z.-Q. & Li, J. Improved operational stability of blue phosphorescent OLEDs by functionalizing phenyl-carbene groups of tetradentate Pt(II) complexes. *Adv. Funct. Mater.* **34**, 2405066 (2024).
12. Zhang, Y., Lee, J. & Forrest, S. R. Tenfold increase in the lifetime of blue phosphorescent organic light-emitting diodes. *Nat. Commun.* **5**, 5008 (2014).
13. Lee, J. et al. Hot excited state management for long-lived blue phosphorescent organic light-emitting diodes. *Nat. Commun.* **8**, 15566 (2017).
14. Lee, J.-H. et al. Mixed host organic light-emitting devices with low driving voltage and long lifetime. *Appl. Phys. Lett.* **86**, 103506 (2005).
15. Hsiao, C.-H. et al. Recombination zone in mixed-host organic light-emitting devices. *Appl. Phys. Lett.* **89**, 163511 (2006).
16. Huang, T. et al. Delocalizing electron distribution in thermally activated delayed fluorophors for high-efficiency and long-lifetime blue electroluminescence. *Nat. Mater.* https://doi.org/10.1038/s41563-024-02004-w (2024).
17. Tsuji, H., Mitsui, C. & Nakamura, E. The hydrogen/deuterium isotope effect of the host material on the lifetime of organic light-emitting diodes. *Chem. Commun.* **50**, 14870–14872 (2014).
18. Liu, X. et al. Isotope effect of host material on device stability of thermally activated delayed fluorescence organic light-emitting diodes. *Small Sci.* **1**, 2000057 (2021).
19. Yao, J., Dong, S.-C., Tam, B. S. T. & Tang, C. W. Lifetime enhancement and degradation study of blue OLEDs using deuterated materials. *ACS Appl. Mater. Interfaces* **15**, 7255–7262 (2023).
20. Wang, P. et al. Synthesis of all-deuterated tris(2-phenylpyridine)iridium for highly stable electrophosphorescence: the "deuterium effect". *J. Mater. Chem. C.* **1**, 4821–4825 (2013).
21. Li, W. et al. Improved efficiency and stability of red phosphorescent organic light-emitting diodes via selective deuteration. *J. Phys. Chem. Lett.* **13**, 1494–1499 (2022).
22. Abe, T., Miyazawa, A., Konno, H. & Kawanishi, Y. Deuteration isotope effect on nonradiative transition of fac-tris (2-phenylpyridinato) iridium (III) complexes. *Chem. Phys. Lett.* **491**, 199–202 (2010).
23. Bae, H. J. et al. Protecting benzylic C-H bonds by deuteration doubles the operational lifetime of deep-blue Ir-phenylimidazole dopants in phosphorescent OLEDs. *Adv. Optical Mater.* **9**, 2100630 (2021).
24. Huang, T. et al. Enhancing the efficiency and stability of blue thermally activated delayed fluorescence emitters by perdeuteration. *Nat. Photonics* **18**, 516–523 (2024).
25. Lu, T. & Chen, Q. Shermo: A general code for calculating molecular thermochemistry properties. *Comput. Theor. Chem.* **1200**, 113249 (2021).
26. Wang, D., Cheng, C., Tsuboi, T. & Zhang, Q. Degradation mechanisms in blue organic light-emitting diodes. *CCS Chem.* **2**, 1278–1296 (2020).
27. Wang, R., Meng, Q.-Y., Wang, Y.-L. & Qiao, J. Negative charge management to make fragile bonds less fragile toward electrons for robust organic optoelectronic materials. *CCS Chem.* **4**, 331–343 (2022).
28. Lee, H. J., Lee, H. L., Han, S. H. & Lee, J. Y. Novel secondary acceptor based molecular design for superb lifetime in thermally activated delayed fluorescent organic light-emitting diodes through high bond energy and fast up-conversion. *Chem. Eng. J.* **427**, 130988 (2022).
29. Shen, P.-C., Zhuang, Z.-Y., Zhao, Z.-J. & Tang, B.-Z. Recent advances of folded tetraphenylethene derivatives featuring through-space conjugation. *Chin. Chem. Lett.* **27**, 1115–1123 (2016).
30. Shen, P. et al. Achieving efficient multichannel conductance in through-space conjugated single-molecule parallel circuits. *Angew. Chem., Int. Ed.* **59**, 4581–4588 (2020).
31. Li, J. et al. Mechanical single-molecule potentiometers with large switching factors from ortho-pentaphenylene foldamers. *Nat. Commun.* **12**, 167 (2021).
32. Jagtap, S. P. & Collard, D. M. Multitiered 2D π-stacked conjugated polymers based on pseudo-geminal disubstituted [2.2]paracyclophane. *J. Am. Chem. Soc.* **132**, 12208–12209 (2010).
33. Wang, X.-Q. et al. Multi-layer π-stacked molecules as efficient thermally activated delayed fluorescence emitters. *Angew. Chem., Int. Ed.* **60**, 5213–5219 (2021).
34. Shen, P. et al. Through-space conjugated electron transport materials for improving efficiency and lifetime of organic light-emitting diodes. *Adv. Sci.* **9**, 2200374 (2022).
35. Kim, J. et al. Critical role of electrons in the short lifetime of blue OLEDs. *Nat. Commun.* **14**, 7508 (2023).
36. Yersin, H., Rausch, A. F., Czerwieniec, R., Hofbeck, T. & Fischer, T. The triplet state of organo-transition metal compounds. Triplet harvesting and singlet harvesting for efficient OLEDs. *Coord. Chem. Rev.* **255**, 2622–2652 (2011).
37. Thompson, D. W., Fleming, C. N., Myron, B. D. & Meyer, T. J. Rigid medium stabilization of metal-to-ligand charge transfer excited states. *J. Phys. Chem. B* **111**, 6930–6941 (2007).
38. Schmidbauer, S., Hohenleutner, A. & König, B. Chemical degradation in organic light-emitting devices: mechanisms and implications for the design of new materials. *Adv. Mater.* **25**, 2114–2129 (2013).
39. Chai, J.-D. & Gordon, M. H. Long-range corrected hybrid density functionals with damped atom–atom dispersion corrections. *Phys. Chem. Chem. Phys.* **10**, 6615–6620 (2008).
40. Kronik, L., Stein, T., Refaely-Abramson, S. & Baer, R. Excitation gaps of finite-sized systems from optimally tuned range-separated hybrid functionals. *J. Chem. Theory Comput.* **8**, 1515–1531 (2012).
41. Sun, H., Zhong, C. & Brédas, J. L. Reliable prediction with tuned range-separated functionals of the singlet–triplet gap in organic emitters for thermally activated delayed fluorescence. *J. Chem. Theory Comput.* **11**, 3851–3858 (2015).
42. Martin, R. L. Natural transition orbitals. *J. Chem. Phys.* **118**, 4775–4777 (2003).
43. Neese, F. The ORCA program system. *WIREs Comput. Mol. Sci.* **2**, 73–78 (2012).
44. Frisch, M. J. et al. *Gaussian 16, Revision C.01* (Gaussian, Inc., Wallingford, CT, 2016).

45. Scott, A. P. & Radom, L. Harmonic vibrational frequencies: an evaluation of Hartree-fock, møller-plesset, quadratic configuration interaction, density functional theory, and semiempirical scale factors. *J. Phys. Chem.* **100**, 16502–16513 (1996).
46. Hess, B., Kutzner, C., Van der Spoel, D. & Lindahl, E. GROMACS 4: Algorithms for highly efficient, load-balanced, and scalable molecular simulation. *J. Chem. Theory Comput.* **4**, 435–447 (2008).
47. Van der Spoel, D. et al. GROMACS: Fast, flexible, and free. *J. Comput. Chem.* **26**, 1701–1718 (2005).

Acknowledgements

This work is supported by the National Natural Science Foundation of China (Grant Nos. 52222308 to D.Z. and 22135004 to L.D.), the National Key Research and Development Program (numbers 2022YFB3603002 to T.H. and 2023YFE0203300 to L.D.).

Author contributions

L.D. and D.Z. conceived and supervised this work. D.Z. proposed the molecular design concept and designed the experiments. W.Y. synthesized deuterated materials, carried out the quantum chemical calculations, fabricated and characterized the devices. T.H. and J.Z. helped measure the device performances. M.T. helped revise the paper. L.D., D.Z. and W.Y. discussed the results and wrote and revised the paper with input from all authors.

Competing interests

The authors declare no competing interests.

Additional information

Supplementary information The online version contains supplementary material available at https://doi.org/10.1038/s41467-025-59583-8.

Correspondence and requests for materials should be addressed to Dongdong Zhang or Lian Duan.

Peer review information *Nature Communications* thanks Pi-Tai Chou, Shou-Cheng Dong, and the other, anonymous, reviewer(s) for their contribution to the peer review of this work. A peer review file is available.